Radiotherapy and Oncology 177 (2022) 113–120

Contents lists available at ScienceDirect

Radiotherapy and Oncology

journal homepage: www.thegreenjournal.com

Original Article

Lymph drainage and cervical fascia anatomy-oriented differential nodal CTV delineation at the supraclavicular region for esophageal cancer and nasopharyngeal cancer

Zuxian Zhong [a,b], Dan Wang [b,c], Yi Liu [b,c], Shilong Shao [d], Sihao Chen [b,c], Shanshan He [b,c], Ningjing Yang [e], Churong Li [b], Jing Ren [e], Yue Zhao [b], Qifeng Wang [b], guotai Wang [f], Chuntang Sun [g], Shichuan Zhang [b,c,*]

[a] Graduate School, Chengdu Medical College; [b] Department of Radiation Oncology, Sichuan Cancer Hospital & Institute, School of Medicine, University of Electronic Science and Technology of China, Sichuan Cancer Center, Radiation Oncology Key Laboratory of Sichuan Province, Chengdu; [c] Department of Oncology, Affiliated Hospital of Southwest Medical University, Luzhou; [d] School of Medicine; [e] Department of Radiology, Sichuan Cancer Hospital and Institute, Sichuan Cancer Center, School of Medicine; [f] School of Mechanical and Electrical Engineering, University of Electronic Science and Technology of China; and [g] Department of Obstetrics and Gynecology, Key Laboratory of Birth Defects and Related Diseases of Women and Children(Sichuan University), Ministry of Education, West China Second University Hospital, Sichuan University, Chengdu, China

ARTICLE INFO

Article history:
Received 17 May 2022
Received in revised form 5 October 2022
Accepted 30 October 2022
Available online 3 November 2022

Keywords:
Supraclavicular CTV
Nasopharyngeal cancer(NPC)
Esophageal cancer(EC)

ABSTRACT

Purpose: To determine the differences in supraclavicular lymph node metastasis between esophageal cancer (EC) and nasopharyngeal cancer (NPC) and explore the feasibility of differential supraclavicular clinical target volume (CTV) contouring between these two diseases based on the involvement of different fascial spaces.

Materials and methods: One hundred patients with supraclavicular nodes positive for EC or NPC were enrolled, and their pre-treatment images were reviewed. The distribution patterns of nodes between the two diseases were compared in the context of node levels defined by the 2017 Japanese Esophageal Society and 2013 International Consensus on Cervical Lymph Node Level Classification. Grouping supraclavicular nodes based on sub-compartments formed by the cervical fascia was discussed, and the feasibility of differential CTV contouring based on the differences in the involvement of these sub-compartments between EC and NPC was explored.

Results: The 2013 Consensus on cervical node levels and 2017 Japanese Esophageal Society node station could not practically guide supraclavicular CTV contouring. We divided the supraclavicular space into six sub-compartments: the para-esophageal space (PES), carotid sheath space (CSS), sub-thyroid pre-trachea space (STPTS), pre-vascular space (PVS), and vascular lateral space (VLS) I and II. EC mainly spread to the PES, STPTS, CSS, and VLS I, whereas NPC tended to spread to the CSS, VLS I, and VLS II. These combinations of sub-compartments may help constitute the supraclavicular CTVs for EC and NPC.

Conclusions: The fascia anatomy-based sub-compartments sufficiently distinguished metastasis to the supraclavicular space between EC and NPC, thus facilitating differential CTV contouring between these two diseases.

The supraclavicular region is unique; it can show the involvement of malignancies from the head and neck as well as the thorax and lower body [1]. The lymph flow of the entire body converges into the thoracic duct at the left neck and the lymphatic duct at the right neck and finally empties into the venous system in this region. Thus, metastatic cells in enlarged lymph nodes in this region can be disseminated from any site of the body. For head and neck, upper esophageal, and breast cancers, the supraclavicular region is an integral part of the nodal clinical target volume (CTV) for prophylactic purposes. Studies on lymph node distribution in this region for individual malignancies have been reported, and proposals for CTV contouring have been made by independent authors [2–6].However, to date, no comparative study has attempted to discuss the differences in the nodal spread pattern in this region among different cancers and the pathophysiological basis underlying these differences.

The cervical fascia is a thin layer of fibrous connective tissue that separates the muscles and organs of the neck into different compartments [7–9]. Its development can be traced back to weeks 6–12 of the embryonic stage [10–12]. Although the terminology

* Corresponding author at: Department of Radiation Oncology, Sichuan Cancer Hospital & Institute, School of Medicine, University of Electronic Science and Technology of China, Sichuan Cancer Center, Radiation Oncology Key Laboratory of Sichuan Province, Chengdu, China.
E-mail address: zhangsc65@hotmail.com (S. Zhang).

https://doi.org/10.1016/j.radonc.2022.10.036
0167-8140/

and detailed histological analyses of cervical fascia are still developing [13,14], its importance in understanding disease spread and the rationale for the surgical procedure has been well recognized. The cervical lymph nodes are closely related to the anatomy of the cervical fascia. Deep cervical lymph nodes are lined in the compartment formed by the superficial and deep layers of deep cervical fascia (DCF). We have previously reported that the boundaries of level IIb CTV of nasopharyngeal cancer (NPC) can be determined on the basis of the anatomical landmarks of this compartment at the upper neck [15]. In the supraclavicular region, this lymph node-containing compartment can be further divided into several sub-compartments by the carotid sheath and visceral fascia that encompasses the central line organs (the esophagus, thyroid, and trachea). Lymph flow from above and beneath the clavicle may involve these sub-compartments differentially, which may lead to differences in the enrollment of these sub-compartments into CTV coverage.

In this study, we sought to explore the spatial relationship between lymph node distribution and these sub-compartments and attempted to provide explanations for the distinctions among different malignancies from the perspective of the lymph drainage pathway and cervical fascia anatomy. We used esophageal cancer (EC) and NPC as representative malignancies of the lower neck/thorax and upper neck, respectively. Both malignancies show a high frequency of supraclavicular metastases.

Material and methods

Patients and images

This study was approved by the Ethics Committee of Sichuan Cancer Hospital (SCH; approval number: SCCHEC-02–2022-03). The requirement for individual consent for this retrospective analysis was waived. Images of consecutive patients histologically diagnosed with EC or NPC in 2020 at SCH were retrospectively reviewed by ZS, YN, and RJ until 100 cases each of EC and NPC with positive lymph nodes in the supraclavicular region were identified. The cranial edge of the supraclavicular region is defined as the caudal border of the cricoid bone, and the caudal edge is defined as the level at which the subclavian vein (SCV) converges into the internal jugular vein (IJV). Patients with previous treatment and synchronous secondary malignancies were excluded from the study. The criteria for positive nodes were as follows: 1) short diameter $\geq$ 10 mm; 2) short diameter < 10 mm but significantly responsive to treatment (maximum diameter reduced by half); 3) node at the peri-esophageal space (between the carotid sheath and esophagus/bronchus) with a short diameter $\geq$ 5 mm; and 4) three or more clustered lymph nodes, with a maximum short diameter $\geq$ 8 mm [16]. Cervical EC and thoracic EC with cervical extension were excluded because lymph drainage of these tumors may involve both the thoracic and cervical lymph networks. We also excluded patients with NPC without level II or III metastasis even if they had enlarged supraclavicular nodes because "skipped" cervical metastasis is rare in NPC [5]. Pre-treatment contrast-enhanced computed tomography (CT) and magnetic resonance (MR) images were used for node distribution analysis. The protocols for image acquisition have been described previously [15].

Analysis of the distribution patterns of lymph nodes according to the node level defined by the 2013 international consensus and 2017 Japanese esophageal society

To account for any potential spread, positive nodes as well as other nodes $\geq$ 3 mm (equal to the slice thickness of axial CT and MR images) were marked to provide a full picture of node distribution in the supraclavicular region, and all nodes were further categorized into 3–8 mm, 8–10 mm, and > 10 mm groups based on the risk of involvement. On the basis of their spatial relationship to the adjacent organs, including the blood vessels, esophagus, trachea, thyroid, and scalene muscles, nodes were mapped as representative small circles with a 3 mm diameter to a template simulative CT for head and neck cancer. The position of the geometric center of each node was determined under consensus by ZS, YN, and RJ.

Both the 2013 International Cervical Node Level Consensus and 2017 Japanese Esophageal Cancer Diagnosis and Treatment Guidelines have defined node levels (stations) of the supraclavicular region from the perspective of head and neck cancer and EC, respectively [17–19]. To validate the practical value of these systems in guiding CTV contouring, the distribution of lymph nodes within each node level defined by the 2013 Consensus and 2017 Japanese Esophageal Society (JES) was analyzed, and the node numbers within each level were calculated.

Definition of supraclavicular sub-compartments on the basis of fascial anatomy and lymph node distribution pattern and proposal of nodal CTV delineation for EC and NPC

The literature on cervical fascial anatomy was carefully reviewed. Several sub-compartments within the supraclavicular region have been proposed according to the spatial relationship between fasciae and cervical structures in the supraclavicular region. The frequency of the nodes plotted within these sub-compartments was calculated. Individual sub-compartments were evaluated as a CTV component based on the nodal involvement risk for EC and NPC. Thus, different CTV coverages would be determined based on different sub-compartment combinations.

Results

Clinical characteristics of the patients

Pre-treatment images of 944 patients with NPC and 620 patients with EC admitted in 2020–2021 were reviewed until 100 cases with positive supraclavicular nodes were collected. Thus, the incidence of supraclavicular metastasis for NPC and EC could be estimated as 10.6 % and 16.1 %, respectively, which are comparable to the incidence in the literature [20–23]. The characteristics of the patients are summarized in Supplementary Table 1.

Node distribution pattern at the supraclavicular region and its spatial relationship to node level of the 2013 consensus and 2017 JES

A total of 470 nodes for NPC (3–8 mm, 318; 8–10 mm, 68; and $\geq$ 10 mm, 84) and 291 nodes for EC (3–8 mm, 168; 8–10 mm, 39; $\geq$10 mm, 84) were identified for analysis. The supraclavicular region lymph node distribution of NPC and EC by the 2013 Consensus and 2017 JES are summarized in different tables (Supplementary Tables 2 and 3) and illustrated with several representative planes in Fig. 1 (see the full image in Supplementary Figs. 1–4).

For NPCs, levels IV and V defined by the 2013 Consensus cover 92.77 %, 88.16 %, and 85.71 % of all identified nodes with diameter $\geq$ 3 mm, diameter $\geq$ 8 mm, and diameter $\geq$ 10 mm. Other nodes were observed within level VIb and a space posterior and lateral to level Vb-c, which was previously not defined by the 2013 Consensus (Fig. 1A, Supplementary Fig. 1, Supplementary Table 2).

Within level VIb (peri-esophageal space), a total of four nodes (two with 3–8 mm, one with 8–10 mm, and one with $\geq$ 10 mm diameter) from three patients were identified. Among these three patients, two had multiple enlarged nodes near the carotid sheath, suggesting that their level VIb metastasis likely spread from the

Table 1
The boundaries of the six fascia-determined sub-compartmental spaces.

Subgroup	Boundaries					
	Cranial	**Caudal**	**Anterior**	**Posterior**	**Medial**	**Lateral**
Pre-vascular space (PVS)	Caudal edge of cricoid cartilage	Caudal edge of venous angle (SCV joints with IJV)	Posterior edge of SCM	Anterior edge of CCA and IJV	Lateral edge of strap muscle	Posterior edge of SCM
Carotid sheath space (CSS)	Caudal edge of cricoid cartilage	Caudal edge of venous angle (SCV joints with IJV)	Anterior edge of CCA and IJV	Anterior edge of pre-vertebral muscle	Medial edge of CCA, vertebral artery	Lateral edge of IJV
Vascular lateral space I (VLS I)	Caudal edge of cricoid cartilage	Caudal edge of venous angle (SCV joints with IJV)	Posterior edge of the SCM; Line connects anterior edge of IJV and OHM, when OHM appear;	Anterior edge of the pre-vertebral muscle	Lateral edge of IJV	Lateral edge of SCM
Vascular lateral space II (VLS II)	Caudal edge of cricoid cartilage	Caudal edge of venous angle (SCV joints with IJV)	Line connects SCM and TM, at upper planes; OHM, when OHM appears; Extension line of anterior edge of IJV, at lower planes	Anterior edge of scalene muscle	Lateral border of SCM	Medial edge of TM, at upper planes; Middle point of anterior edge of LSM, when OHM appears, at lower planes
Para-esophageal space (PES)	Caudal edge of cricoid cartilage	Caudal edge of venous angle (SCV joints with IJV)	Posterior edge of lateral lobe of thyroid; Extension line of anterior edge of CCA, plane inferior to thyroid	Anterior edge of prevertebral muscles and vertebral arteries	Lateral edge of esophagus and trachea	Medial border of CCA
Sub-thyroid pre-trachea space (STPTS)	Caudal edge of thyroid	Caudal edge of venous angle (SCV joints with IJV)	Posterior edge of SM	Anterior edge of trachea	Lateral edge of trachea	Extension line of anterior edge of IJV and CCA

Abbreviations: CCA, common carotid artery; IJV, internal jugular vein; LSM, levator scapulae muscle; OHM, omohyoid muscle; SCM, Sternocleidomastoid muscle; SCV, subclavian artery; SM, strap muscles; TM, trapezius muscle.

adjacent level IV nodes. One patient with a solitary level VIb node (8 mm diameter and responded to treatment) had limited lower neck metastasis (three positive nodes within IV and V in total), thus representing unpredictable metastasis to level VIb in NPC.

A total of 30 nodes (14, 5, and 11 with diameters of 3–8 mm, 8–10 mm, and ≥ 10 mm, respectively) from 18 patients were observed at the posterior/lateral space to levels Vb and Vc. This space was not defined by either the 2013 Consensus or the 2017 CTV International Guidelines for NPC [24]. However, metastasis to this region is not rare in NPC and has been reported by several authors [5,25]. Here, we adopted the definition of PLV proposed by Jiang et al. for this space for the convenience of discussing node distribution in this region. The distribution of cervical lymph nodes in patients with lymph node metastases at the PLV level is summarized in Supplementary Table 4.

We also analyzed the coverage of nodes on the basis of the 2017 JES levels. The node levels or node stations defined by the 2017 JES are from the perspective of surgery rather than CTV contouring in radiotherapy. The boundaries of each station were not well-defined in the CT images. We tried contouring levels 101, 104, and 106 according to the definitions in the 2017 JES guidelines and related literature [3,19,26,27].The lateral boundaries of 104 defined by the guidelines are pre-accessory nerves, which cannot be identified by either CT or MR imaging. We arbitrarily divided 104 into 104a (medial part) and 104b (lateral part) according to the lateral edge of the sternocleidomastoid muscle (SCM). Among these, l04b extends laterally until it meets the trapezius muscle (TM) and clavicle, and 99.15 %, 98.68 %, and 98.80 % of NPC nodes with diameters ≥ 3 mm, ≥ 8 mm, and ≥ 10 mm were found to be predominantly located within levels 104a and 104b (Fig. 1B, Supplementary Fig. 2, Supplementary Table 3). As mentioned previously, four nodes from three patients were located exceptionally close to the esophagus (three in l01 and 1 in 106rec).

Unlike NPC, nodes of the EC were mainly found near the esophagus and carotid sheath. Level IV, level VIa, and level VIb of the 2013 Consensus cover 95.53 % of all nodes and 100 % of the positive nodes and those ≥ 8 mm (Fig. 1D, Supplementary Fig. 3, Supplementary Table 2). Fourteen nodes (4.47 % of all nodes) from eight patients were detected at level V (11 nodes) and PLV (two nodes). These nodes were all small in size (3–8 mm). Most of them (10 nodes from five patients) had no accompanied level IV enlarged nodes (≥8 mm), suggesting that they were likely reactive lymphadenopathy rather than tumor-related nodes. In the JES station system, JES levels 104a, 106pre, 106ac, and 101 cover all positive nodes and nodes with a high risk of involvement (8–10 mm). The 13 small nodes located in level V and PLV were covered by station 104b (Fig. 1E, Supplementary Fig. 4, Supplementary Table 3).

Taken together, the findings imply that EC tends to spread to the space adjacent to the esophagus and carotid sheath, whereas NPC mainly spreads to the space lateral to the carotid sheath, with rare peri-esophageal involvement. Apparently, some levels/stations defined either by the 2013 Consensus or 2017 JES as supraclavicular level have plenty of void spaces that are rarely involved by EC and NPC, which warrants further cropping of these levels to optimize the CTV for each disease.

Proposal of sub-compartments at the supraclavicular region based on the lymph drainage pathway and cervical fascia anatomy

The superficial layer of the deep cervical fascia (SDCF), middle layer of the deep cervical fascia (MDCF), deep layer of the deep cervical fascia (DDCF) or prevertebral fascia (PF), and alar fascia (AF)

in the supraclavicular region divide this region into several subspaces, which may have important implications in the compartmentation of lymph node groups [7,8,28]. However, these fasciae are not visible in CT or MR images because of their limited thickness in histology. Representative lines for these fasciae, which were determined by the edges of anatomical structures that these fasciae cover or enclose, were drawn to define the boundaries of these subspaces.

The position at which the AF attaches to the PF has not been well-documented in the literature. Histological studies have shown that this position may vary among individuals and even between the left and right sides of the same individual [28,33]. We found that the vertebral vein may serve as a landmark for this position (Fig. 2). Nearly 99.15 % of the metastatic nodes of NPC are located lateral to the line drawn between the medial edge of the carotid sheath and vertebral vein.

The SCM, TM, and levator scapulae muscle (LSM) serve as good landmarks for the lateral boundary of the upper supraclavicular space regarding lymph drainage. The lateral boundary of the lower part is not well-defined by the 2017 JES or 2013 Consensus. Lin et al. suggested that the inferior belly of the omohyoid muscle (OHM) can be used as the lateral boundary of the CTV because there were no nodes at the lateral side of the OHM [20]. In agreement with Lin et al., we also found that all but one enlarged node was present within the medial side of OHM. This exceptional node has a size of 4.4 × 4.7 mm and is derived from an NPC patient with multiple metastases in level Vb. At planes close to the clavicle bone, as a landmark of the anterior border, the SCM is replaced by the strap muscles (SM). The OHM and SM are both enclosed by MDSF (Fig. 2).

Six fascia-determined sub-compartmental spaces were established: the para-esophageal space (PES), sub-thyroid pre-tracheal space (STPTS), carotid sheath space (CSS), pre-vascular space (PVS), vascular lateral space (VLS) I, and VLS II. The boundaries of these spaces are described in Table 1 and Fig. 2.

The positive nodes of NPCs were predominantly located in the CSS, VLS I, and VLS II (Fig. 1C, Supplementary Figure 5, and Supplementary Table 5). No nodes were found within the PVS and STPTS, and only four nodes were found in the PES (in Lin's study, only two nodes with diameters of 3–8 mm were found in this region). As described before, PES involvement likely occurs as a result of extensive metastasis to the CSS and VLS I. It should be safe to omit PES from the prophylactic CTV for NPC when the CSS is not involved. We found that the lower portion of VLS II (inferior to the transverse cervical vessel, which is the caudal border of Vb as per the 2013 Consensus) contained a limited number of enlarged nodes (≥8 mm) (Fig. 1, A2-A4, Fig. 3B, Supplementary Figure 5, E9-E19), and below the plane wherein the inferior belly of OHM appears (Fig. 1, A3 and A4, Supplementary Figure 5, E13-E19), even small nodes (3–8 mm) were not found within VLS II. Thus, for CTV contouring, when VLS II has a low risk of involvement (no positive nodes in level Va, proposed VLS I, and CSS), VLS II can be tailored to

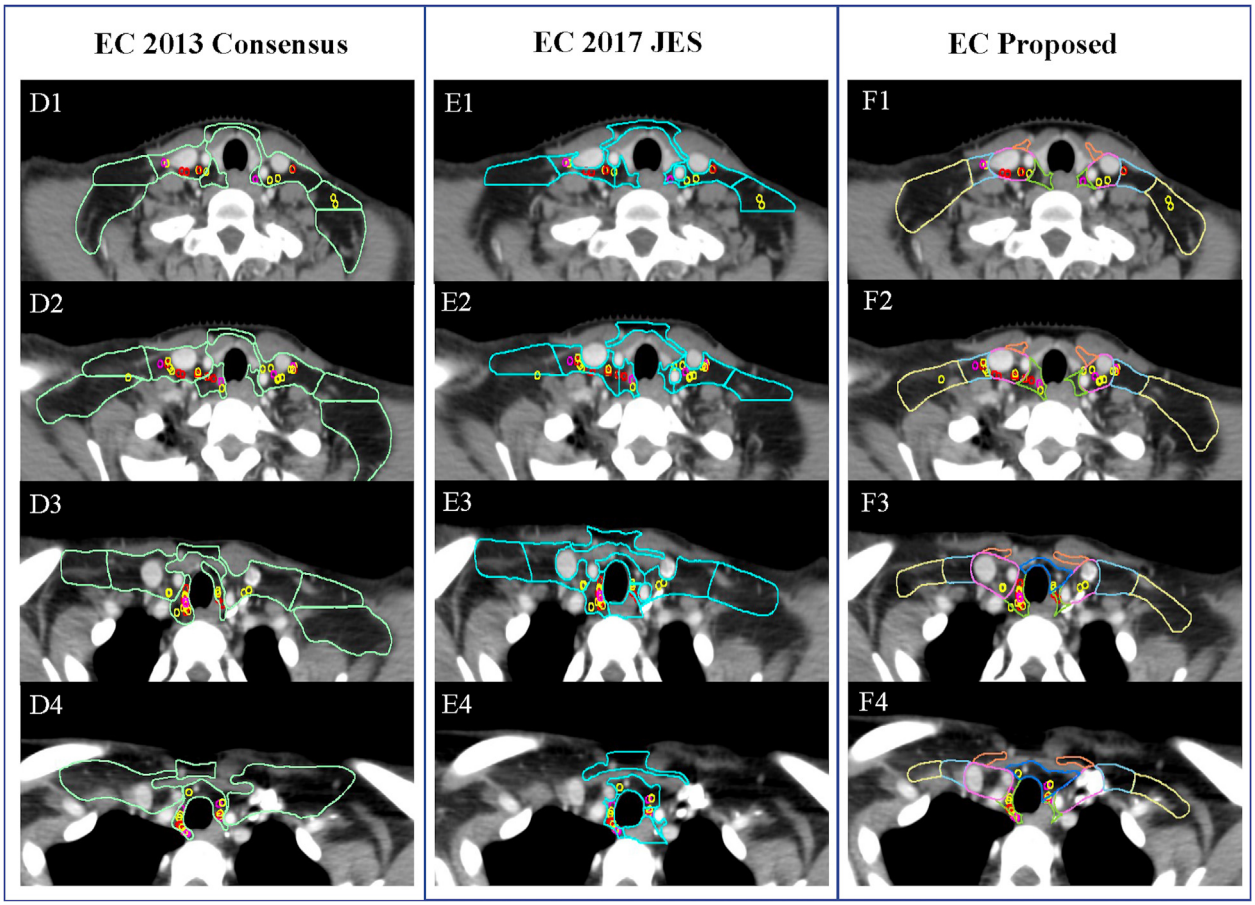

Fig. 1. Distribution of lymph nodes at the supraclavicular space in nasopharyngeal cancer and esophageal cancer, displayed in four transverse sections at different planes. A1–4 and D1-4, the distribution pattern of nodes on the basis of the 2013 International Consensus on Cervical Node Level (2013 Consensus, hereafter); B1–4 and E1-4, the distribution pattern of nodes on the basis of the 2017 Japanese Esophagus Diagnosis and Treatment Guidelines (2017 JES); C1–4 and F1-4, the distribution pattern of nodes on the basis of the proposed six fascia anatomy-based sub-compartments. Abbreviations: NPC, nasopharyngeal cancer; EC, esophageal cancer; PES, para-esophageal space; STPTS, sub-thyroid pre-tracheal space; CSS, carotid sheath space; PVS, pre-vascular space; VLS, vascular lateral space.

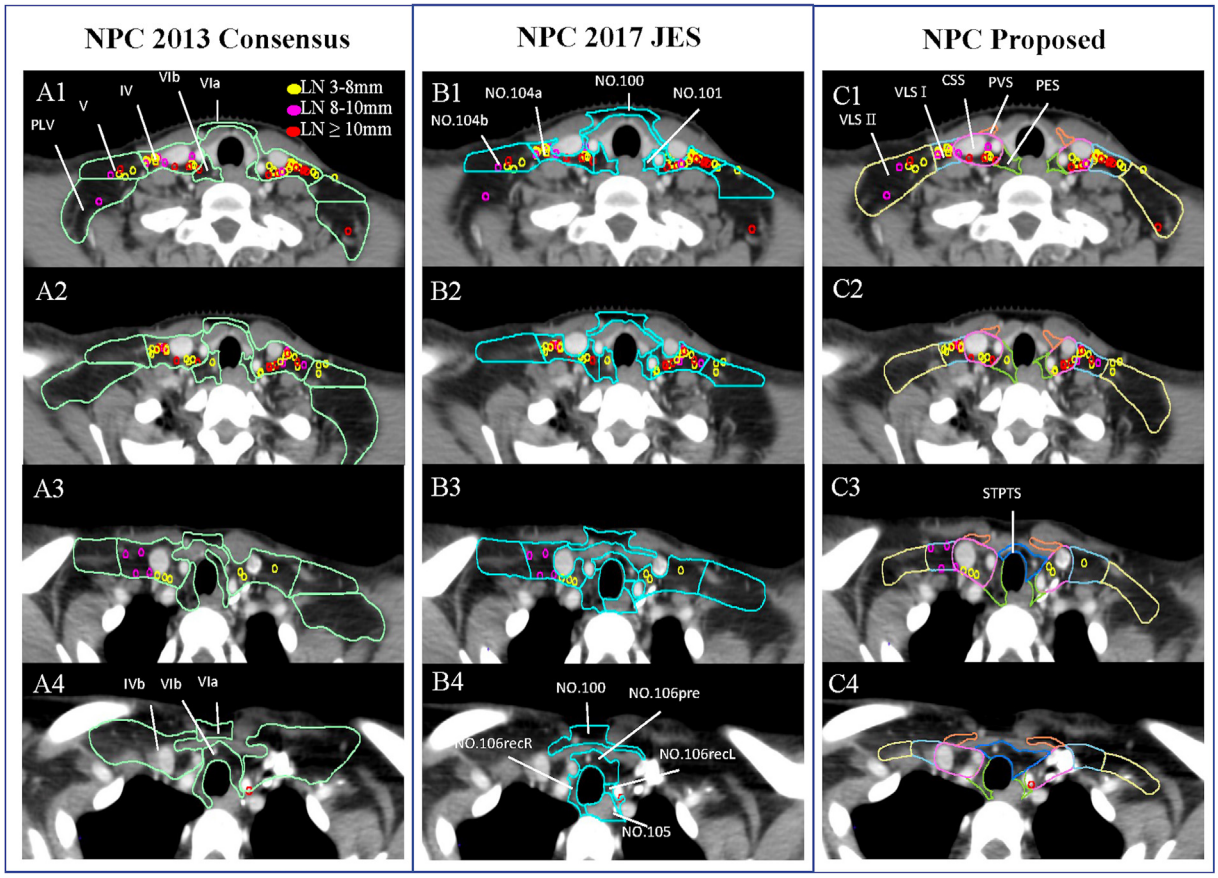

Fig. 1 (*continued*)

include its upper part above the transverse vessels. At planes below the inferior belly of OHM, VLS II may be spared even with the presence of the above-mentioned risk factors (Fig. 4, B5, Supplementary Figure 7, H15, and H16).

The caudal border of the supraclavicular CTV of NPC deserves discussion because it has not been clearly defined by any guidelines or discussed elsewhere. We investigated several layers below the SCV (planes that are lower than the caudal border of the supraclavicular region defined by the current study) and found no single nodes under the SCV, even for the three patients with PES involvement. Therefore, we suggest that the cranial border of the SCV could be used as the caudal border of the CTV in NPC (Fig. 2B, Fig. 4, A5, and B5, Supplementary Figure 7, G16, and H16). It is conceivable that the drainage node of the upper neck is normally situated above the venous angle.

In contrast with NPCs, the positive nodes and high-risk nodes (≥8 mm) of EC were all found within the CSS, PES, VLS I, and lateral portion of STPTS (Fig. 1F, Supplementary Table 6, Supplementary Figure 6). As mentioned previously, only 13 small nodes were found in VLS II. The CTV for EC requires routine coverage of PES, VLS I, and the lateral portion of STPTS, whereas VLS II can be considered when VLS I contains positive nodes. At planes below the inferior belly of OHM, the CTV can be further tailored to include PES and STPTS (Fig. 4C, see full image in Supplementary Figure 7).

Notably, most positive nodes of EC were found within the lower part of the supraclavicular space, particularly close to the thoracic duct and venous angle (Fig. 3). We measured the distance between the center point of all recorded lymph nodes and the caudal edge of the jugular venous angle. The distance between the lymph node and jugular venous angle in the left neck was 20.06 ± 12.28 mm (mean ± SD, node of all sizes) and 18.51 ± 12.83 mm (positive nodes and nodes ≥ 8 mm), and that in the right neck was 17.66 ± 12.55 mm and 14.37 ± 10.57 mm. *De novo* metastasis of thoracic EC to levels above the cricoid bone is rare, especially without supraclavicular metastasis; thus, for both sides, 30 mm above the venous angle would be sufficient to cover 95 % of the potential metastatic nodes of EC in the supraclavicular region (Fig. 3C, Fig. 4, C3, Supplementary Figure 7, J9).

Discussion

To date, no study has specifically discussed CTV contouring in the supraclavicular region. In 2017, an international consensus on CTV delineation for NPC, a practical guide for CTV contouring, was proposed, and it included the supraclavicular region [24]. However, these CTVs were based on the node level defined for head and neck cancer [17]. Their feasibility was carefully evaluated by Lin et al. in a detailed analysis of the lymph node distribution of 959 cases of NPC [20]. Subsequently, Lin et al. proposed multiple modifications, including omission of the PVS and usage of the OHM as the lateral boundary for the lower neck. However, the authors did not provide any pathophysiological explanation, making these modifications difficult to understand. Similarly, efforts have been made to optimize the CTV for EC based on the node group defined by the JES [2,3,29]. The inclusion of the spaces around the esophagus and carotid sheath is well-documented among independent studies, but no interpretation has been provided by either of these studies.

The cervical fascia divides the neck space into multiple compartments. These compartments normally form a longitudinal space that extends from the cranial base to the mediastinum. Evaluation of the relationship between the lymph drainage pathway

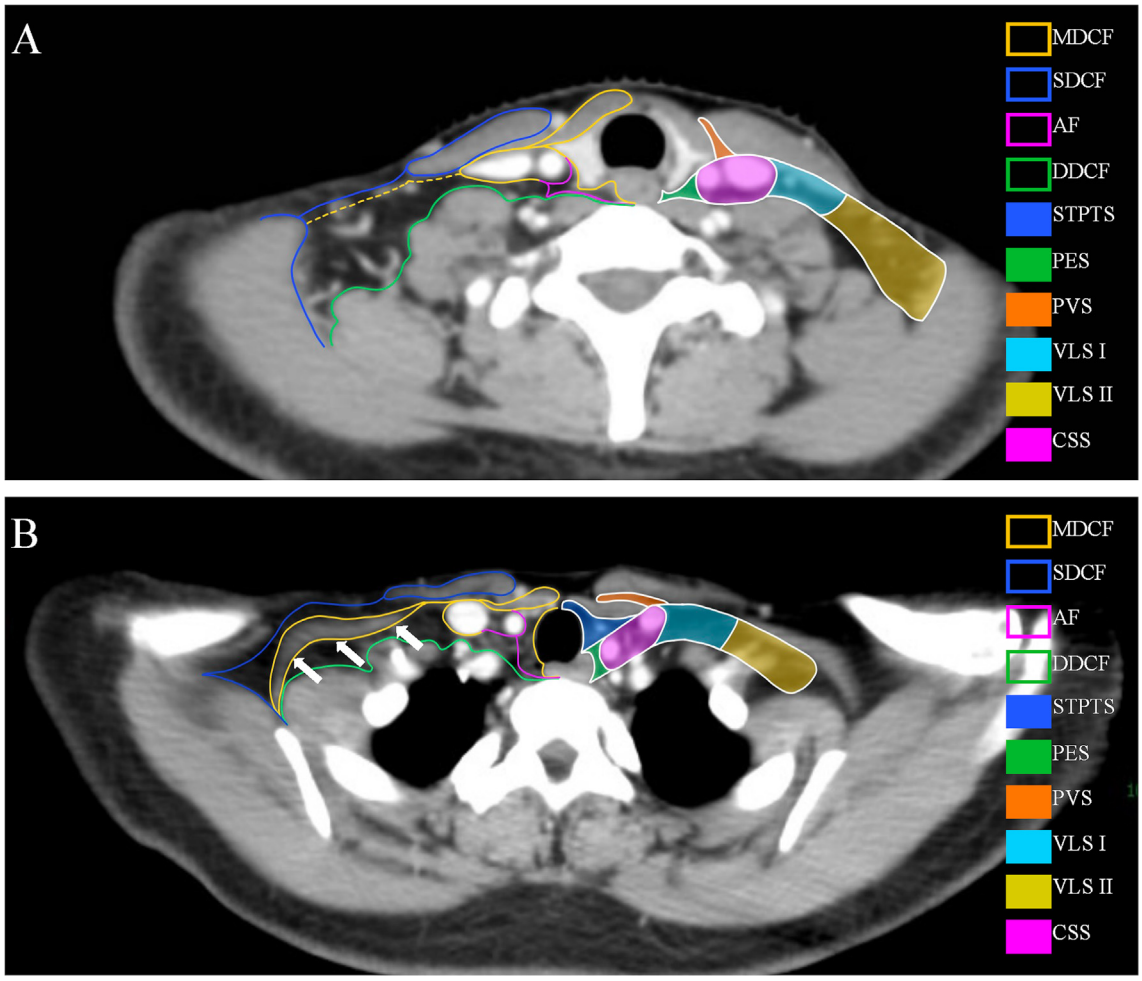

Fig. 2. Cervical fascia anatomy at the supraclavicular space and illustration of the proposed six fascia anatomy-based sub-compartments at two representative transverse sections (A, upper plane of the supraclavicular space; B, lower plane of the supraclavicular space, with the presence of the inferior belly of omohyoid muscle). The cervical fascia cannot be seen on either computer-aided tomography or magnetic resonance images but can be outlined according to the border of structures they cover or sheathe. Right side of A and B, cervical fascia anatomy; Left side of A and B, proposed sub-compartments. Note that in A, the lateral part of the middle layer of the deep cervical fascia is drawn as a dotted line because it has not been well-documented in the literature. Abbreviations: SDCF, superficial layer of deep cervical fascia; MDCF, middle layer of deep cervical fascia; DDCF, deep cervical fascia; AF, alar fascia; PES, para-esophageal space; STPTS, sub-thyroid pre-trachea space; CSS, pink for carotid sheath space; PVS, pre-vascular space; VLS, vascular lateral space. White arrow, the omohyoid muscle.

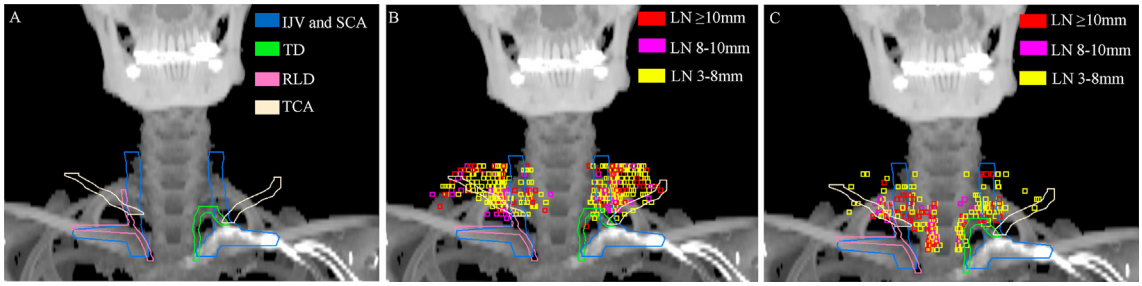

Fig. 3. Spatial relationship between lymph nodes and important landmark structures is shown in the frontal view of the three-dimensional reconstruction of images. A, landmark structures; B, node distribution of nasopharyngeal cancer in the supraclavicular space. The enlarged lymph nodes found in nasopharyngeal cancer patients in the supraclavicular space spread from the IJV to the medial edge of the trapezius but converge toward the RLD and TD at the lower planes, likely following the drainage pathway of TCA chain. C, node distribution of esophageal cancer at the supraclavicular space. The nodes of esophageal cancer can be divided into two groups as para-esophagus and peri-thoracic duct. They may receive lymph flow through different pathways, one through the longitudinal lymph network of the esophagus and the other through TD or RLD. Abbreviations: IJV, internal jugular vein; SCA, subclavian artery; RLD, right lymphatic duct; TD, thoracic duct.

and fascia-defined compartments may provide an anatomical rationale for optimizing CTV coverage. The findings of the current study clearly demonstrated that among the six sub-compartments formed by the cervical fascia in the supraclavicular region, NPC and EC showed distinct involvement patterns, which facilitated differential CTV coverage for NPC and EC.

Knowledge of the drainage pathways of lymph flow for NPC and EC is essential for understanding the differences in CTV coverage

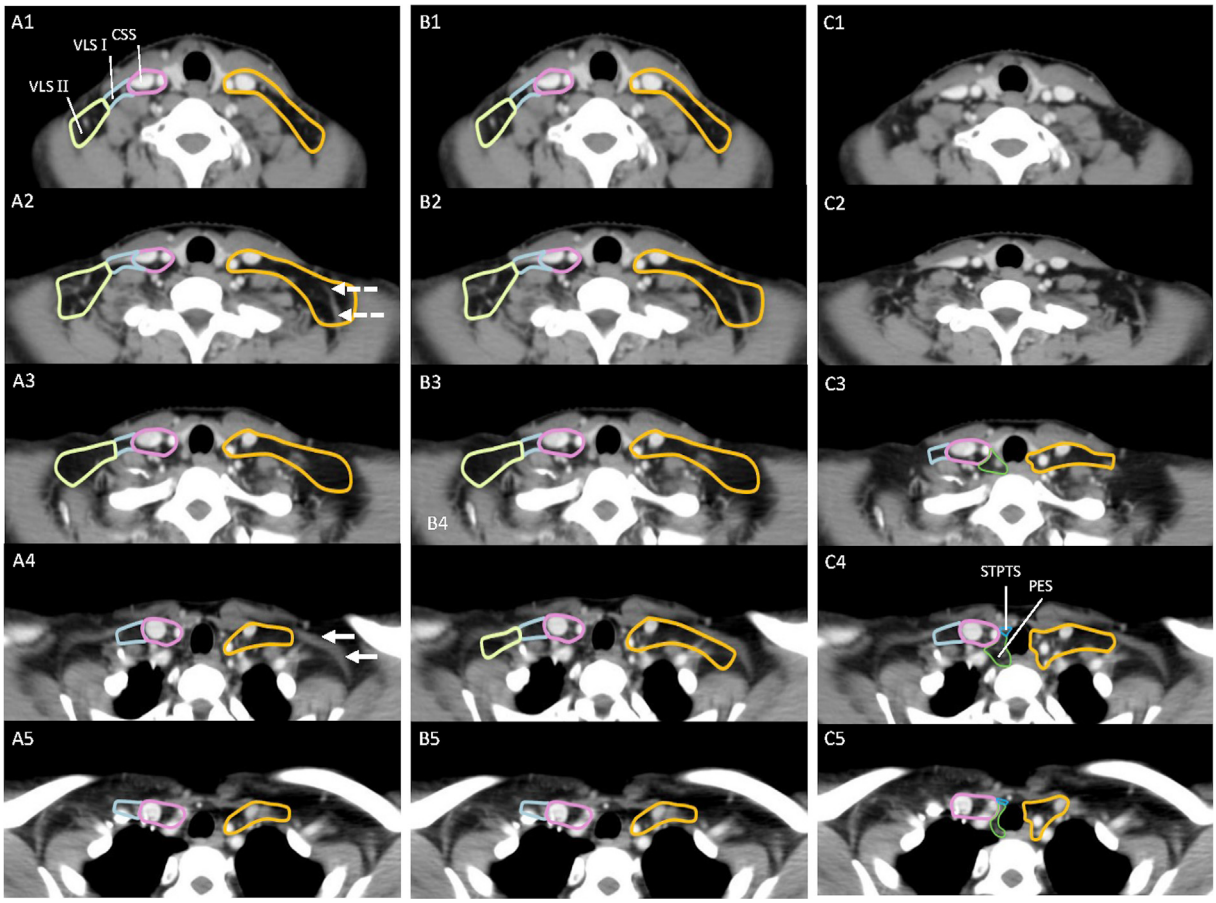

Fig. 4. Nodal CTV delineation for supraclavicular space based on cervical fascia anatomy, displayed in five transverse sections at different planes. A1-5, proposed CTV for patients with nasopharyngeal cancer with a low risk of VLS II metastasis (without positive nodes in level Va, proposed space CSS, and VLS I). VLS II can be omitted for planes below the transverse cervical vessels; B1-5, proposed CTV for patients with nasopharyngeal cancer with a high risk of VLS II metastasis (with involvement of level Va, proposed space CSS, and VLS I). VLS II should be covered for these patients, however, at planes below the inferior belly of omohyoid muscle, VLS II can still be spared; C1-5, proposed CTV for patients with thoracic esophageal cancer. The caudal border of CTV can be set about 3 cm above the venous angle. VLS I, PES and lateral portion of the STPTS should be included. At planes below the inferior belly of omohyoid muscle, VLS I can be omitted. White solid arrow, the omohyoid muscle; white dashed arrow, the transverse cervical vessels.

between them [30–32]. Lymph flow from the nasopharynx normally goes through the internal jugular chain anteriorly and the accessory chain posteriorly. The jugular chain descends along the jugular vein and finally merges into the jugular collecting trunk and thoracic duct (lymphatic duct on the right side). In the medial direction, the carotid sheath and AF may act as histological barriers to prevent disease spread from the lateral space to the peripharyngeal and peri-esophageal spaces, making them landmarks for the medial border of the CTV for NPC. Although the accessory chain has branches extending laterally and posteriorly to the front edge of the TM and LSM, it will finally collect all branches and go anteriorly (likely through the transverse chain, Fig. 3, Fig. 4B), merge to the collecting trunk, then converge to the thoracic duct or lymphatic duct, and finally empty into the venous angle [31,32]. The thoracic duct/lymphatic duct and venous angle are both located deep to the SDCF and MDCF [33–35],which may explain why the MDCF-covered OHM and strap muscle may serve as anterior and lateral borders of the supraclavicular compartment at the lower portion of the supraclavicular region.

The drainage pathways for EC are completely different. Lymph nodes in the PES collect lymph fluid directly from the cervical esophagus (sentinel node) [36] and longitudinal lymph vessel network of the middle and upper thoracic esophagus, which accounts for the high occurrence of PES metastasis in EC [36–39]. The sum of the frequency of metastases to CSS and VLS I is greater than that to the PES, suggesting that these metastases might originate from an independent drainage pathway instead of a stepwise spread from PES. This drainage pathway is likely to pass through the thoracic duct (lymphatic duct on the right side). The thoracic duct runs along the left side of the esophagus and receives lymph drainage in the mediastinum; at the clavicular level, it bends anteriorly and laterally, forming an arc, merges with the cervical lymphatic trunk, and is finally injected into the venous angle formed by the SCV and jugular vein [33–35,40–42]. The thoracic duct on the right side collects lymph flow in the upper-right quadrant body and is injected into the right venous angle [31]. On both sides, a collection of lymph nodes and multiple lymphatic branches are situated around the thoracic duct/lymphatic duct [43].These nodes and lymphatic vessels usually have a direct connection with the thoracic duct/lymphatic duct, which may be the major metastatic target of tumor cells spread from the thoracic duct/lymphatic duct. As proof, we found that the distance between positive nodes and the caudal border of the venous angle at the left neck was about 18 mm (would be approximately 12–15 mm excluding the thickness of the SCV), which is very close to the vertical distance of the apex of the thoracic duct to the point it empties into the venous angle (mean, 15.00 mm, by Ammar K et al.; the value of y2s minus y3s in their study) [44].

A limitation of the current study is that this was an observational study with single-center data. Although the major findings have anatomic and physiological support and could be partially validated by other independent studies, a multi-institutional study

with a greater number of patients is still needed to confirm these conclusions. Moreover, the fundamental basis for the compartmentalization effect of the cervical fascia on the lymph vessel network is still lacking. Histological evidence is required in future studies.

In summary, in the current study, we observed distinct patterns of lymph node spread in the supraclavicular region in patients with EC and NPC. We have provided explanations for the differences between these two tumors on the basis of the lymph drainage pathways and detailed anatomy of the thoracic duct/lymphatic duct and cervical fascia. Importantly, we proved that using subcompartments formed by cervical fascia could appropriately group supraclavicular nodes, and joining the individual subcompartments could help determine the coverage of CTV. These CTVs would be different in nature between EC and NPC due to the distinct drainage pathways in EC and NPC and the anatomical barriers formed by the network of cervical fascia.

Funding

This work was supported by the Sichuan Science and technology Foundation Project, China (Grant No. 2022YFSY0055), and Chengdu Science and technology Foundation Project, China (Grant No. 2021-YF05-02390-SN).

Declaration of Competing Interest

The authors declare that they have no known competing financial interests or personal relationships that could have appeared to influence the work reported in this paper.

Appendix A. Supplementary material

Supplementary data to this article can be found online at https://doi.org/10.1016/j.radonc.2022.10.036.

References

[1] Masaomi., Mizutani M, Shin-ichi., et al. Anatomy and histology of Virchow's node. *Anatomical Science International* 2005
[2] Liu M, Chen Y, Fu X, Zhao K, Jiang GL. Proposed revision of CT-based cervical and thoracic lymph node levels for esophageal cancer in UICC 7th version. Radiother Oncol 2014;113:175–81.
[3] Luo Y, Liu Y, Wang X, et al. Mapping patterns of nodal metastases in esophageal carcinoma: rethinking the clinical target volume for supraclavicular nodal irradiation. J Thorac Dis 2016;8:3132–8.
[4] Wang Y, Ye D, Kang M, et al. Mapping of cervical and upper mediastinal lymph node recurrence for guiding clinical target delineation of postoperative radiotherapy in thoracic esophageal squamous cell carcinoma. Front Oncol 2021;11:663679.
[5] Wang X, Hu C, Ying H, et al. Patterns of lymph node metastasis from nasopharyngeal carcinoma based on the 2013 updated consensus guidelines for neck node levels. Radiother Oncol 2015;115:41–5.
[6] Li L, Li Y, Zhang J, et al. Optimization of cervical lymph node clinical target volume delineation in nasopharyngeal carcinoma: a single center experience and recommendation. Oncotarget 2018;9:26980–9.
[7] Guidera AK, Dawes PJ, Fong A, Stringer MD. Head and neck fascia and compartments: no space for spaces. Head Neck 2014;36:1058–68.
[8] Natale G, Condino S, Stecco A, Soldani P, Belmonte MM, Gesi M. Is the cervical fascia an anatomical proteus? Surg Radiol Anat 2015;37:1119–27.
[9] Stecco C, Pirri C, Fede C, et al. Dermatome and fasciatome. Clin Anat 2019;32:896–902.
[10] Lopez-Fernandez P, Murillo-Gonzalez J, Arraez-Aybar LA, de la Cuadra-Blanco C, Moreno-Borreguero A, Merida-Velasco JR. Early stages of development of the alar fascia (human specimens at 6–12 weeks of development). J Anat 2019;235:1098–104.
[11] Miyake N, Takeuchi H, Cho BH, Murakami G, Fujimiya M, Kitano H. Fetal anatomy of the lower cervical and upper thoracic fasciae with special reference to the prevertebral fascial structures including the suprapleural membrane. Clin Anat 2011;24:607–18.
[12] Tokairin Y, Nakajima Y, Kawada K, et al. Histological study of the thin membranous structure made of dense connective tissue around the esophagus in the upper mediastinum. Esophagus 2018;15:272–80.
[13] Feigl G, Hammer GP, Litz R, Kachlik D. The intercarotid or alar fascia, other cervical fascias, and their adjacent spaces - a plea for clarification of cervical fascia and spaces terminology. J Anat 2020;237:197–207.
[14] Guidera AK, Dawes PJD, Stringer MD. Cervical fascia: a terminological pain in the neck. ANZ J Surg 2012;82:786–91.
[15] Zhang J, Pan L, Ren J, et al. Level IIb CTV delineation based on cervical fascia anatomy in nasopharyngeal cancer. Radiother Oncol 2015;115:46–9.
[16] van den Brekel M, Stel H, Castelijns J, et al. Cervical lymph node metastasis: assessment of radiologic criteria. Radiology 1990;177:379–84.
[17] Gregoire V, Ang K, Budach W, et al. Delineation of the neck node levels for head and neck tumors: a 2013 update. DAHANCA, EORTC, HKNPCSG, NCIC CTG, NCRI, RTOG, TROG consensus guidelines. *Radiother Oncol* 2014; 110: 172-81.
[18] 18. Japan Esophageal S. Japanese Classification of Esophageal Cancer, 11th Edition: part II and III. *Esophagus* 2017; 14: 37-65
[19] Japan Esophageal S. Japanese Classification of Esophageal Cancer, 11th Edition: part I. *Esophagus* 2017; 14: 1-36
[20] Lin L, Lu Y, Wang XJ, et al. Delineation of neck clinical target volume specific to nasopharyngeal carcinoma based on lymph node distribution and the international consensus guidelines. Int J Radiat Oncol Biol Phys 2018;100:891–902.
[21] Wu SG, Dai MM, He ZY, et al. Patterns of regional lymph node recurrence after radical surgery for thoracic esophageal squamous cell carcinoma. Ann Thorac Surg 2016;101:551–7.
[22] Taniyama Y, Nakamura T, Mitamura A, et al. A strategy for supraclavicular lymph node dissection using recurrent laryngeal nerve lymph node status in thoracic esophageal squamous cell carcinoma. Ann Thorac Surg 2013;95:1930–7.
[23] Luo Y, Wang X, Liu Y, et al. Identification of risk factors and the pattern of lower cervical lymph node metastasis in esophageal cancer: implications for radiotherapy target delineation. Oncotarget 2017;8:43389–96.
[24] Lee AW, Ng WT, Pan JJ, et al. International guideline for the delineation of the clinical target volumes (CTV) for nasopharyngeal carcinoma. Radiother Oncol 2018;126:25–36.
[25] Jiang C, Gong B, Gao H, et al. Correlation analysis of neck node levels in 960 cases of Nasopharyngeal carcinoma (NPC). Radiother Oncol 2021;161:23–8.
[26] Schuring N, Matsuda S, Hagens ERC, et al. A proposal for uniformity in classification of lymph node stations in esophageal cancer. Dis Esophagus 2021;34.
[27] Huang W, Huang Y, Sun J, et al. Atlas of the thoracic lymph nodal delineation and recommendations for lymph nodal CTV of esophageal squamous cell cancer in radiation therapy from China. Radiother Oncol 2015;116:100–6.
[28] Weijs TJ, Goense L, van Rossum PSN, et al. The peri-esophageal connective tissue layers and related compartments: visualization by histology and magnetic resonance imaging. J Anat 2017;230:262–71.
[29] Yu J, Ouyang W, Li C, et al. Mapping patterns of metastatic lymph nodes for postoperative radiotherapy in thoracic esophageal squamous cell carcinoma: a recommendation for clinical target volume definition. BMC Cancer 2019;19:927.
[30] Werner JA, Dunne AA, Myers JN. Functional anatomy of the lymphatic drainage system of the upper aerodigestive tract and its role in metastasis of squamous cell carcinoma. Head Neck 2003;25:322–32.
[31] Lengele B, Hamoir M, Scalliet P, Gregoire V. Anatomical bases for the radiological delineation of lymph node areas. major collecting trunks, head and neck. Radiother Oncol 2007;85:146–55.
[32] Wang Y, Ow TJ, Myers JN. Pathways for cervical metastasis in malignant neoplasms of the head and neck region. Clin Anat 2012;25:54–71.
[33] Wedel T, Heinze T, Moller T, et al. Surgical anatomy of the upper esophagus related to robot-assisted cervical esophagectomy. Dis Esophagus 2021;34.
[34] Johnson OW, Chick JF, Chauhan NR, et al. The thoracic duct: clinical importance, anatomic variation, imaging, and embolization. Eur Radiol 2016;26:2482–93.
[35] Liu ME, Branstetter BFt, Whetstone J, Escott EJ. Normal CT appearance of the distal thoracic duct. *AJR Am J Roentgenol* 2006; 187: 1615-20
[36] Mizutani M, Murakami G, Nawata S, Hitrai I, Kimura W. Anatomy of right recurrent nerve node: why does early metastasis of esophageal cancer occur in it? Surg Radiol Anat 2006;28:333–8.
[37] M. R, . VV, M. S. The lymphatic drainage of the esophagus. *Bulletin De Lassociation Des Anatomistes* 1993; 77: 33
[38] Wang Y, Zhu L, Xia W, Wang F. Anatomy of lymphatic drainage of the esophagus and lymph node metastasis of thoracic esophageal cancer. Cancer Manag Res 2018;10:6295–303.
[39] Kuge K, Murakami G, Mizobuchi S, Hata Y, Aikou T, Sasaguri S. Submucosal territory of the direct lymphatic drainage system to the thoracic duct in the human esophagus. J Thorac Cardiovasc Surg 2003;125:1343–9.
[40] Kammerer FJ, Schlude B, Kuefner MA, et al. Morphology of the distal thoracic duct and the right lymphatic duct in different head and neck pathologies: an imaging based study. Head Face Med 2016;12:15.
[41] Nomura T, Niwa T, Ozawa S, Oguma J, Shibukawa S, Imai Y. The visibility of the terminal thoracic duct into the venous system using MR thoracic ductography with balanced turbo field echo sequence. Acad Radiol 2019;26:550–4.
[42] Phang K, Bowman M, Phillips A, Windsor J. Review of thoracic duct anatomical variations and clinical implications. Clin Anat 2014;27:637–44.
[43] Murakami G, Sato T, Takiguchi T. Topographical anatomy of the bronchomediastinal lymph vessels: their relationships and formation of the collecting trunks. Arch Histol Cytol 1989;53:219–35.
[44] Ammar K, Tubbs RS, Smyth MD, et al. Anatomic landmarks for the cervical portion of the thoracic duct. *Neurosurgery* 2003; 53: 1385-7; discussion 7-8.